

# Pyrolysis kinetics of hydrochars produced from brewer's spent grains

M. P. Olszewski<sup>1</sup>, P. A. Maziarka<sup>2</sup>, P. J. Arauzo<sup>1</sup>, F. Ronsse<sup>2</sup>, A. Kruse<sup>1</sup>

\* corresponding author: maciej.olszewski@uni-hohenheim.de

<sup>1</sup>Department of Conversion Technologies of Biobased Resources, Institute of Agricultural Engineering, University of Hohenheim, Garbenstrasse 9, DE-70599 Stuttgart, Germany

<sup>2</sup>Department of Green Chemistry and Technology, Faculty of Bioscience Engineering, Ghent University, Coupure Links 653, 9000 Gent, Belgium

## Abstract

The aim of the study was to understand pyrolysis behavior and estimate the kinetic parameters (activation energy and pre-exponential factor A) of the pyrolysis of different hydrochars produced from brewer's spent grains (BSG). To achieve this, non-isothermal thermogravimetric analysis at different heating rates (5, 10, 20, 40 °C min<sup>-1</sup>) in the temperature range 40-900 °C and with constant nitrogen flow (70 mL min<sup>-1</sup>) was carried out. The measurements were conducted for the BSG and three hydrochars produced from BSG at different HTC conditions: (i) 180 °C, 4 h; (ii) 220 °C, 2 h; and (iii) 220 °C, 4h. The kinetic parameters were estimated using the Kissinger-Akahira-Sunose (KAS) method. The average activation energy was 285 kJ mol<sup>-1</sup> for BSG and 147, 170, 188 kJ mol<sup>-1</sup> for the hydrochars. Also, BSG and three hydrochars were pyrolyzed at 300, 500, 700, and 900 °C. The yields of the pyrolyzed materials and the elemental analysis were measured and compared with the raw biomass and hydrochars to evaluate changes in composition induced by the pyrolysis process. Moreover, pyro GC-MS analysis was applied to characterize volatile matter released during BSG and its hydrochars decomposition.

## Keywords

hydrothermal carbonization, pyrolysis, kinetics, hydrochar, biomass, spent grain

## Highlights

- The HTC process reduces material input for pyrolysis proportionally to HTC yield
- The HTC process used before pyrolysis essentially increased the pyrolysis yields

- Hydrochars showed lower pyrolysis activation energy compared to initial biomass

## 1. Introduction

According to statistics [1], beer is classified at 3<sup>rd</sup> position of the most popular drinks worldwide (after water and tea). The global production of beer reached 196 billion (10<sup>9</sup>) liters in 2016 [1,2]. During the production of beer, residues are generated, mostly brewer's spent grains (BSG). It is estimated that every 1 liter of beer leads to 0.14-0.20 kg of wet BSG (20-30 wt. % dry matter), which results in the annual production of 27-39 mln ton wet BSG worldwide [3,4].

BSG may show different composition, depending on barley species and brewing technology. It is reported [5,6] that BSG (wt. % dry matter) consists of hemicellulose (21.8-40.2), cellulose (12.0-12.54), lignin (4.0-27.8), lipids (3.9-13.3) and proteins (14.2-26.7). Due to high protein and fiber content, BSG is attractive as feed for cattle, as which it currently is mostly used. However, the vast quantities produced by large breweries cannot be used only in this way. The high moisture content of wet BSG increase the transportation costs significantly. This may cause difficulties as well as high costs in delivery for longer distances and results in utilization by local farmers. On the other hand, brewer's spent grains are a lignocellulosic waste biomass stream, which may be valorized in biotechnology and *via* thermochemical conversion. Furthermore, wet biomass causes problems during the storage because it is exposed to microbial attacks and fast growth of bacteria. To avoid this biomass should be dried to a moisture level below 10 wt. % [3,4,7,8] for storage.

Drying of raw biomass is a high energy demanding process; therefore, it is necessary to consider the improvement of energy efficiency. Hydrothermal carbonization process (HTC) of biomass is a thermochemical process, during which biomass is converted into a solid product, using liquid water in the subcritical conditions as the reaction medium. The process operates at elevated

temperature (180-260 °C) and pressure (above water vapor pressure to keep medium in the liquid phase) [7,9–14]. The HTC process allows expanding the potential range of biomass application for bioenergy purposes since the drying step of raw biomass is avoided.

Consequently, it is possible to convert troublesome wet biomass containing from 70 up to 90 wt. % of water, for example, bio-waste streams (wastewater sludge, bio-refinery digestate, pulp and paper sludge) and food production leftovers (brewer's spent grains, sugar beet bagasse, fruit pomace) using HTC [7,10,14–17]. The HTC product, also known as hydrochar, is more hydrophobic than the precursor [9]. Hence, it may be more efficient mechanically dewatered to moisture contents as low as 50 wt. %, depending on used methods, to be more susceptible to drying [18]. The HTC process also reduces the amount of material which has to be dried, proportionally to HTC yield. It results in a more economically and energetically efficient process, due to reduced drying stages and saving the heat necessary to evaporate water from the hydrochars.

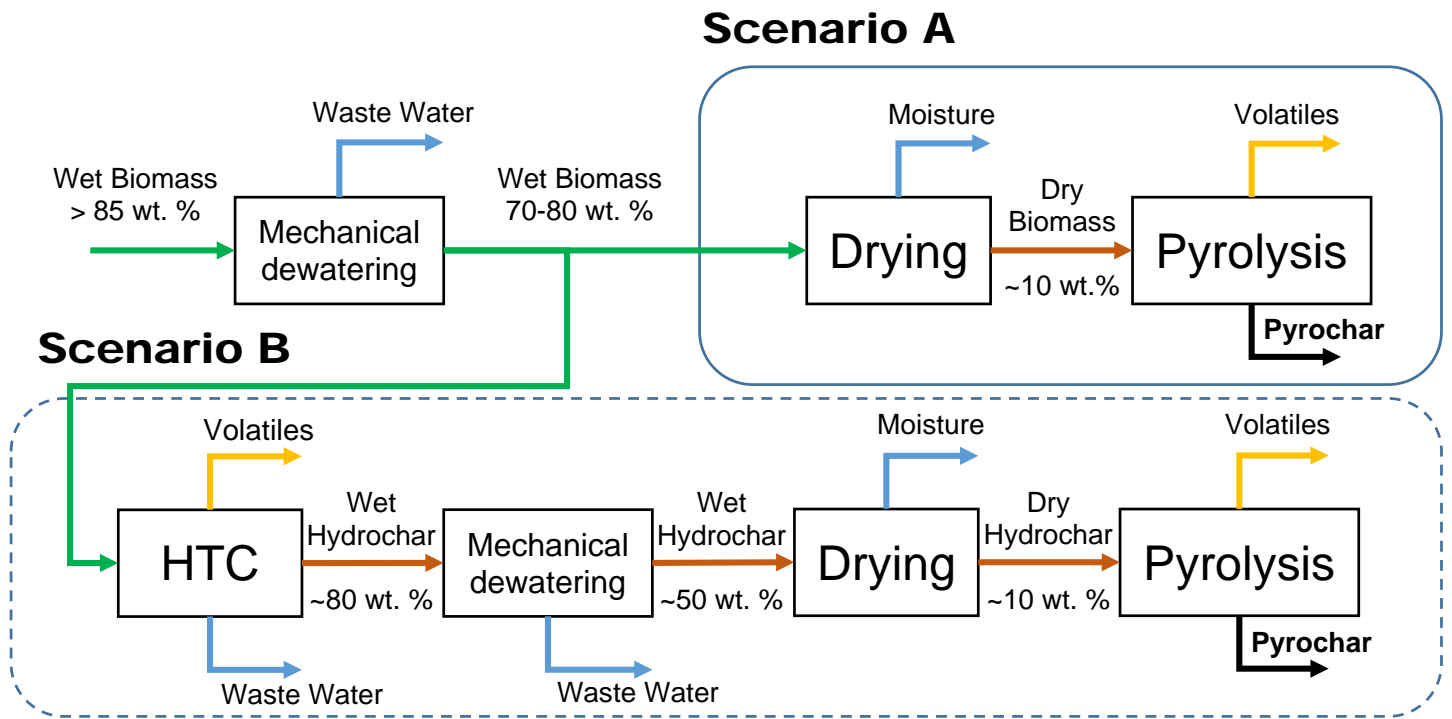


**Fig. 1.** Simplified process flow diagram; Scenario A – Conventional Pyrolysis, Scenario B the integration of HTC with Pyrolysis.

A subsequent pyrolysis process can be coupled to treat hydrochar (Fig. 1, Scenario B) in order to further increase its carbon content, calorific value, surface area and to decrease its phytotoxicity. Fresh hydrochar may have a toxic effect on plant growth [19]. As a result, the final char can be used in a broader range of applications, for example, electricity generation in CHP plant, soil improvement, hydrogen and chemicals production, activated carbons production, carbon-rich materials for supercapacitors and carbon electrodes, and as a reductant in the metallurgical industry [18–20].

For all those purposes fundamental pyrolysis study of global pyrolysis kinetics of hydrochars is necessary to understand the thermal degradation. The hydrochars were produced in three different process conditions: (i) 180 °C, 4 h residence time; (ii) 220 °C, 2 h; and (iii) 220 °C, 4 h to investigate the effect of HTC process variables on the hydrochars decomposition behavior during the pyrolysis process. The kinetic parameters (activation energy and pre-exponential factor) were estimated based on Kissinger-Akahira-Sunose (KAS) method. The initial biomass and hydrochars were pyrolyzed at 300, 500, 700, and 900 °C using TGA. Additionally, the proximate and ultimate analysis of obtained chars were carried out and compared with initial materials.

## 2. Methodology

### 2.1. Materials

The brewer's spent grains (BSG) used as feedstock in this research was delivered by neighborhood brewery Hoepfner (Karlsruhe, Germany). Oven-dried (at 105 °C) biomass was ground to particle size below 200 µm. Then the material was named as BSG and stored in a plastic zip bag. Three hydrochars were produced using wet BSG (22 wt. % moisture) at different process conditions: 1) 180 °C, 4 h residence time; 2) 220 °C, 2 h residence time; and 3) 220 °C and 4 h residence time. Obtained hydrochars were named as HTC-180-4, HTC-220-2, and HTC-220-4, respectively. The hydrochars were dried overnight at 105 °C, next ground to a particle size below 200 µm and kept in plastic zip bags. More detailed information about feedstock preparation and hydrochars production was described elsewhere [21].

### 2.2. TGA – DSC experiment

TGA – DSC analyses were performed for the BSG and hydrochars produced at different conditions using a Netzsch STA Jupiter 449 F5 (Germany). The samples were placed in alumina crucibles and heated up to 105 °C then kept over 10 min in isothermal condition to remove moisture from the samples. Afterward, samples were heated up to temperature 900 °C using four different heating rates 5, 10, 20 and 40 °C min<sup>-1</sup> to achieve a non-isothermal degradation for further kinetic analysis [22–24]. The nitrogen gas with a flow of 70 mL min<sup>-1</sup> was used to provide an inert atmosphere during the pyrolysis process. To avoid mass and heat transfer limitation around 5 mg of sample was evenly spread in the crucible [25]. All measurement was carried out in triplicates.

Additionally, a series of pyrolysis experiments with a heating rate of 10 °C min<sup>-1</sup> were conducted for BSG and hydrochars. The samples were heated up from ambient temperature to 300, 500, 700, and 900 °C and held 10 min at desired temperature. The pyrolysis yield, as well as the

elemental composition of produced pyrochars, were analyzed. For this purpose, 40 mg of sample was used to obtain enough material for the analysis.

### 2.3. Proximate and ultimate analysis

Elemental analysis of the raw BSG, hydrochars and pyrochars was performed on CHNS analyzer EuroEA, 3000 Serie (HEKAtech GmbH, Germany) according to the standard (DIN-51732). The oxygen content was calculated from the difference between the combined mass of measured elements in the dry ash-free basis. The moisture content, volatile matter (VM) and ash content for raw BSG and hydrochars were conducted according to industrial standard (ASTM-D1762-84). The difference between the sum of measured ash and VM contents from 100% is the value of fixed carbon (FC) [24]. The measurements were made in duplicates; the average data were reported. The ash content for pyrochars because of a small amount of the samples was calculated assuming that all ash from the initial substrate stays in the final product. The VM of pyrochars was calculated based on the difference between the sample and the reference char obtained at 900 °C. The higher heating value (HHV, MJ kg<sup>-1</sup>) was calculated based on Channiwala and Parikh equation (Eq. 1) [26]. The formula is widely used because of its high accuracy. Additionally, it may be used for a wide range of fuels including solid, liquid and gases.

$$HHV = 0.3491C + 1.1783H + 0.1005S - 0.1034O - 0.0151N - 0.021A \quad (1)$$

where, C, H, S, O, N, A refer to carbon, hydrogen, sulfur, oxygen, nitrogen, and ash contents, respectively (wt. %).

#### 2.4. A mathematical model for the pyrolysis kinetics

To describe the pyrolysis kinetic one-step global model can be used [24,27,28]. The model assumes that the process occurs as a single reaction, where the feedstock is converted to char (solid residue) with releasing of volatiles (gas and bio-oil) as shown below [27].



To analyze the TGA data is necessary to use a mathematical model. The solid material decomposition rate can be described as follow:

$$\frac{d\alpha}{dt} = k(T)f(\alpha) \quad (3)$$

where,  $f(\alpha)$  is a conversion function which depends on the reaction mechanism, and  $d\alpha/dt$  is the conversion rate of the feedstock over the reaction time  $t$ . Conversion ( $\alpha$ ) is calculated by the following expression:

$$\alpha = \frac{m_0 - m_t}{m_0 - m_f} \quad (4)$$

where,  $m_0$ ,  $m_t$ ,  $m_f$  corresponds to initial mass of the feedstock, mass after reaction time  $t$ , and final remaining mass after the process, respectively.

$k(T)$  is reaction rate constant depended on the temperature and is described by the fundamental Arrhenius equation:

$$k(T) = A \exp\left(-\frac{E_A}{RT}\right) \quad (5)$$

where,  $A$  is the pre-exponential factor [ $s^{-1}$ ],  $E_A$  is the activation energy [ $J \text{ mol}^{-1}$ ],  $R$  is the universal gas constant [ $J \text{ K}^{-1} \text{ mol}^{-1}$ ], and  $T$  is temperature [ $K$ ].

In non-isothermal thermogravimetric analysis temperature (T) is increasing linearly with known heating rate ( $\beta$ ) over the time (t), which is represented as follow:

$$\beta = \frac{dT}{dt} \quad (6)$$

Subsequently, by substituting equations (4) and (5) into equation (2), the differential form of non-isothermal decomposition is obtained:

$$\frac{d\alpha}{dT} = \frac{A}{\beta} \exp\left(-\frac{E_A}{RT}\right) f(\alpha) \quad (7)$$

Finally, by the integration of Eq. 7 for the initial condition  $T = T_0$  and  $\alpha = 0$  results in the fundamental equation which is a basis for all kinetic methods to determine the kinetic parameters during the pyrolysis process:

$$\int_0^\alpha \frac{d\alpha}{f(\alpha)} = g(\alpha) = \frac{A}{\beta} \int_{T_0}^T \exp\left(-\frac{E_A}{RT}\right) dT \quad (8)$$

The expression of the reaction mechanism as a function in derivative [ $f(\alpha)$ ] or integral [ $g(\alpha)$ ] form could be found elsewhere [29]. Many methods were proposed by researchers to solve this complex phenomenon. Coats and Redfern [30] developed a model-fitting method (CR) to describe the reaction mechanism. Kinetic parameters could also be determined by isoconversional (model-free) methods established by Kissinger [31], Friedman [32], Flynn-Wall-Ozawa (FWO) [33,34], Kissinger-Akahira-Sunose (KAS) [35]. The model-free methods allow skipping the choice of reaction mechanism in the calculation which eliminates an associated error [36].

## 2.5. Calculation of pyrolysis kinetics and thermodynamic parameters

In this work to characterize pyrolysis kinetic of brewer's spent grains and its hydrochars KAS method was used. The kinetics calculations were conducted in the temperature range from 105 to 800 °C and different heating rates (5, 10, 20 and 40 °C min<sup>-1</sup>). The technique is expressed as follow:

$$\ln\left(\frac{\beta}{T_{\alpha}^2}\delta\right) = \ln\left(\frac{A_{\alpha}R}{E_{A\alpha}g(\alpha)}\delta\right) - \frac{E_{A\alpha}}{T_{\alpha}R} \quad (9)$$

where  $\beta$ ,  $T_{\alpha}$ ,  $A_{\alpha}$ ,  $E_{A\alpha}$ , and  $\delta$  refer to heating rate [K min<sup>-1</sup>], temperature of desired conversion [K], pre-exponential factor [min<sup>-1</sup>], apparent activation energy [J mol<sup>-1</sup>] for a fixed degree of conversion  $\alpha$  [-], and unit correction factor [K<sup>-1</sup> min<sup>-1</sup>] respectively. The apparent activation energy for a selected degree of conversion was calculated from the slope by plotting  $\ln(\beta/T_{\alpha}^2)$  versus  $1/T_{\alpha}$ .

Additionally, the pre-exponential factors (A) were calculated based on [37]:

$$A = \frac{\beta E_A \exp\left(\frac{E_A}{RT_m}\right)}{RT_m^2} \quad (10)$$

where:  $T_m$  is a DTG peak temperature [K].

Additionally, the activation temperature ( $T_A$ ) [K] was calculated from the following equation:

$$T_A = \frac{E_A}{R} \quad (11)$$

where,  $E_A$  is activation energy [J mol<sup>-1</sup>], and  $R$  is the universal gas constant [J K<sup>-1</sup> mol<sup>-1</sup>].

## 2.6. Statistical data analysis

To calculate activation energy according to KAS method is necessary to use TGA data at different heating rates. Herein, four different HR (5, 10, 20, 40 °C min<sup>-1</sup>) with three replicates (A, B, C) were used. The average temperature from three replicates (AAAA, BBBB, CCCC) for each degree of conversion may be used for the calculation of the activation energy. However, a more precise statistical method due to the larger populations is using the permutation. In this particular case, the permutation with repetitions should be used, where elements  $k=3$  (3-replicates, A, B, C) and the number of  $n$ -tuples= $n$  (4 different heating rates). It results in  $3^n=81$  possible configurations (AAAA, ABAA, ..., CCCC) for the calculation, which provides more accurate and reliable results. The results obtained from the second method were shown as the average values with standard deviation.

### 3. Results and discussion

#### 3.1. Feedstocks characteristic

Three hydrochars (HTC-180-4, HTC-220-2, and HTC-220-4) were produced at different process condition as described in section 2.1. The hydrochars yields were 67.5, 58.0, 55.0 wt. % on dry basis, respectively. Summarized results from the proximate and ultimate analysis of BSG and hydrochars are presented in Table 1. Analyzed materials showed moisture content from 3.25 to 4.06 wt. %, despite earlier drying. It is due to the adsorption of water from the air during processing and storage of the samples. Slight difference between materials may be due to increasing hydrophobicity of hydrochars with the temperature of the HTC process [10]. It follows changes mainly in van der Waals forces in the sorption of water particles. The ash content of the initial biomass was 4.16 wt. % moreover, rose slightly in more severe conditions up to 4.67 wt. % for hydrochar produced at 220°C, and 4 h residence time. On the basis of the yield of hydrothermal carbonization, the ash content of hydrochars was expected to be higher. It means that part of inorganic substances was removed during the process, e.g., dissolving of sodium and potassium salts (carbonates, chlorides and phosphates) [10,17,38,39]. The thermochemical conversion of biomass reduces volatile matter (VM) as well as increase fixed carbon (FC) content into the final product by changing the internal structure. Here, the hydrothermal conversion of brewer's spent grains decreased VM from 76.25 to 61.85 wt. %, which results in increased FC content from 19.59 to 33.48 wt. %. Furthermore, hydrochars had higher carbon and lower oxygen contents than the original biomass caused by dehydration, decarboxylation, condensation, aromatization and polymerization reactions occurring during HTC [9]. It results in a noticeable increase of the estimated HHV for hydrochars (~29.5-31 MJ kg<sup>-1</sup>) which is in the range of lignite (dry ash free basis), and it is higher compared to initial biomass (23.59 MJkg<sup>-1</sup>). Besides, BSG had high protein content [5,6] and hence high nitrogen content in the raw biomass (4.89 wt. %) as well as in the

hydrochars (4.67 wt. %). The nitrogen content is kept approximately at the same level, despite the mass loss of the hydrochars in the conversion process. It means that a part of nitrogen passed into the process water in the form of organic compounds [40].

**Table 1**

*Proximate and ultimate analysis of brewer's spent grains and its hydrochars.*

Analysis	BSG		HTC-180-4		HTC-220-2		HTC-220-4	
Moisture, wt. %	3.75	± 0.65	4.06	± 0.41	3.42	± 0.75	3.25	± 0.83
Proximate analysis, db, wt. %								
Ash	4.16	± 0.05	4.22	± 0.05	4.27	± 0.13	4.67	± 0.13
Volatile Matter	76.25	± 0.07	67.72	± 0.17	65.85	± 0.57	61.85	± 1.03
Fixed Carbon	19.59	± 0.76	28.06	± 0.24	29.88	± 0.63	33.48	± 0.57
Ultimate analysis, daf, wt. %								
C	53.50	± 0.40	66.29	± 0.33	68.82	± 0.75	70.17	± 0.77
H	7.27	± 0.09	7.39	± 0.04	7.62	± 0.05	7.21	± 0.06
N	4.89	± 0.27	4.54	± 0.06	4.61	± 0.06	4.67	± 0.14
S	0.30	± 0.02	0.46	± 0.01	0.45	± 0.01	0.45	± 0.02
O	34.04	± 0.80	21.33	± 0.45	18.51	± 0.65	17.51	± 1.00
HHV, daf, MJ kg <sup>-1</sup>	23.53	0.16	29.54	0.11	30.89	0.25	31.06	0.23

db – dry basis

daf – dry ash-free

### 3.2. Pyrolysis char characteristic

Table 2 presents char yield and proximate and ultimate analysis for pyrochars. The relative error from all measurements was below 5%. In a pyrolysis temperature range of 300–500 °C a significant reduction in the volatiles was noticed, i.e. from 56.5 to 3.9 wt. % for biomass and 40-51.1 to 6.2-8.8 wt. % for hydrochars. It results in energy densification in the char, the HHV for precursor increase from 23.53 to 32.22 MJ kg<sup>-1</sup> at 500 °C. However, for hydrochars, the increase of HHV is not significant. The increase in carbon is compensated by a drop in hydrogen content. The loss of VM also slightly increase the porosity [41]. In this region, the char yield is the highest (up to 78.5 for biomass and 85.8 wt. % for hydrochars at 300 °C). Also, the properties of produced chars limit the potential application. Pyro chars produced at relatively low pyrolysis temperature (300 °C) had high VM content, it results in good reactivity and combustion properties [42,43]. In the case of hydrochar pyrolysis organic compounds from the surface, which cause phytotoxicity can be released. Therefore they can be applied as a solid fuel for heat and electricity generation [42] as well as for soil improvement [17,44]. Increasing the temperature from 500 to 700 °C results in further thermal degradation and decreasing volatile matter to 0.3-3.8 wt. %. It results in a significant increase of the porosity [41] as well as slightly higher heating value 31.5-33 MJ kg<sup>-1</sup>, however, the yield is reduced to 22.3 wt. % for biomass and 30.9-40.2 wt. % for hydrochars. In this range, the produced chars have a small content of volatile matter and sufficient surface area; therefore, they are easily accessible for the activating agent. It makes it a suitable precursor for activated carbons production *via* gasification with steam or CO<sub>2</sub> [45]. In the temperature range 700-900 °C, thermal degradation reached the plateau (Fig. 3A), and the char yields decreased to 22.0, 28.3, 37.4, 45.8 wt. % for BSG, HTC-180-4, HTC-220-2, and HTC-220-4, respectively. Obtained chars have a low content of volatiles. It results in high thermal stability, lower HHV due to a change in the ratio of organic to mineral matter content in the materials, and high fixed carbon content of

81-89.8 wt. %. Antal et al. [46] reported that there is an internal structure change (strong cross-linking and aromatization of the structure) due to the higher carbonization degree, which results in increasing electrical conductivity. These chars are carbon-rich materials which have potential as carbon electrodes [47] and reductant in metallurgical (e.g., silicon and ferrosilicon) industry [48].

**Table 2**

*Pyrolysis char yield and proximate analysis for brewer's spent grains and hydrochars.*

Pyrolysis temperature [°C]	Feedstock	Char yield	dry basis wt. %			FC	HHV MJ kg <sup>-1</sup> dry ash-free
			Ash	VM	FC		
300	BSG	78.5	5.31	56.45	38.24	27.26	
	HTC-180-4	79.4	5.31	51.13	43.56	29.49	
	HTC-220-2	81.0	5.26	43.59	51.15	30.99	
	HTC-220-4	85.8	5.44	40.05	54.51	31.12	
500	BSG	25.9	13.08	6.89	80.03	32.22	
	HTC-180-4	35.8	11.78	7.50	80.72	31.59	
	HTC-220-2	46.2	9.21	8.83	81.96	31.11	
	HTC-220-4	52.0	8.98	6.21	84.80	31.88	
700	BSG	22.3	18.67	0.29	81.03	33.09	
	HTC-180-4	30.9	13.64	2.63	83.74	32.34	
	HTC-220-2	41.2	10.34	3.79	85.87	31.48	
	HTC-220-4	46.2	10.11	0.43	89.46	33.13	
900	BSG	22.0	18.92	-	81.08	32.72	
	HTC-180-4	28.3	14.90	-	85.10	31.94	
	HTC-220-2	37.4	11.39	-	88.61	30.73	
	HTC-220-4	45.8	10.20	-	89.80	30.75	

The van Krevelen diagram (Fig. 2) shows atomic H/C versus O/C ratios for feedstock, hydrochars, and pyrochars produced at 300, 500, 700 and 900 °C. These indicators represent the carbonization degree of lignocellulosic materials; high values are related to low-carbonized materials such as biopolymers (hemicellulose and cellulose) as well as different kind of biomasses.

The lower values of the indicators correspond to more carbonized materials like peats, lignites, coals, and anthracites [15]. The H/C (~1.3) and O/C (~0.2) ratio for hydrochars is in the range of lignite (brown coal). Increasing the pyrolysis temperature to 900 °C shifts the H/C and O/C to lower values, into anthracites range, due to more condensed and aromatic structure formed through the carbonization process. It mimics the natural carbonization process which occurred in the earth's crust for millions of years. As shown in Fig. 2, the O/C and H/C ratios for chars produced at the same pyrolysis temperature are very similar, in the case of higher pyrolysis temperatures.

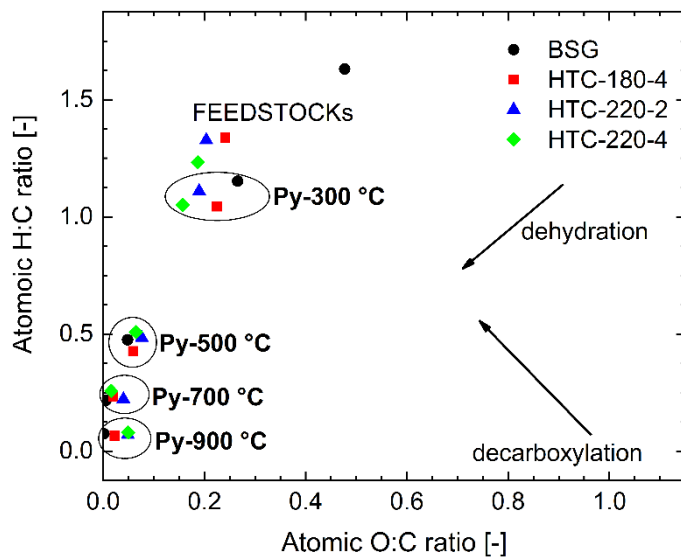


**Fig. 2.** Van Krevelen diagram for feedstocks and pyrochars produced at 300, 500, 700, and 900 °C. Arrows show the ratio changes by the elimination of  $H_2O$  and  $CO_2$ , respectively.

### 3.3. Analysis of TG-DTG curves

The results of the thermogravimetric analysis for BSG and its hydrochars at  $20\text{ }^{\circ}\text{C min}^{-1}$  are shown in Fig. 3. The TG (mass loss) curves and DTG (derivative of TG) as a function of temperature show characteristic tendency associated with the thermal decomposition of lignocellulosic materials. Table A.1 presents such parameters as peaks DTGs and its temperatures as well as final residues (char yields) which are related to the thermal conversion of investigated materials. The TG curve for BSG shows diversity comparing with curves for hydrochars, in the initial stage in the temperature range from 200 to 300  $^{\circ}\text{C}$ . Hydrochars samples begin to decompose at lower temperatures than biomass, which indicates lower thermal stability in this temperature range. This effect is reflected in the DTG curves, where the peak  $\text{DTG}_1$  ( $\sim 293\text{ }^{\circ}\text{C}$ ) is shifted to the left  $\text{DTG}_{1*}$  (lower temperatures, around 230  $^{\circ}\text{C}$ ). Peak  $\text{DTG}_1$  is related to the decomposition of the most reactive biopolymer (hemicellulose 250-330  $^{\circ}\text{C}$ ) which form the structure of biomass [49,50]. During the hydrothermal carbonization process, the hemicellulose is hydrolyzed in temperature around 180  $^{\circ}\text{C}$  [9]. Hence, the peak  $\text{DTG}_{1*}$  may be related with the decomposition of less stable or extreme side parts of the hydrochar structure (e.g., short-chained polymers) created during polymerization of solved molecules during hydrothermal carbonization [16]. On the other hand, the obtained hydrochar was not post-treated after production (e.g., washing with water) and hydrochar is produced under elevated pressure in the liquid environment, which means it could be saturated with organic compounds created during the process (e.g., acetic acid, 5-hydroxymethylfurfural). The second characteristic peak  $\text{DTG}_2$  ( $\sim 360\text{ }^{\circ}\text{C}$ ) is associated with the decomposition of cellulose (350-420  $^{\circ}\text{C}$ ) [51]. The DTG curves (Fig. 3B) for biomass and obtained at different conditions HTC hydrochars shows the unchanged peak for biomass and hydrochar produced at 180  $^{\circ}\text{C}$  and a gradual decrease for materials produced at 220  $^{\circ}\text{C}$  for 2 and 4 hours. It follows that cellulose does not hydrolyze at a temperature of 180  $^{\circ}\text{C}$ , and even at 220  $^{\circ}\text{C}$  does not

undergo complete conversion. It agrees with research published by Kruse et al. [16] and Funke et al. [9] that cellulose starts to hydrolyze at a temperature around 200 °C. The last residual peak DTG<sub>3</sub> (~420 °C) is slightly increased for hydrochars. One of the reasons for this phenomenon could be mass loss related to the thermal degradation of intermediate carbonization products formed during the hydrochar synthesis [16]. On the other hand, it may be due to increased lignin content in hydrochar because of the high stability of lignin during HTC [52]. The TG curves also show a much higher yield of the final char for hydrochars compared to the precursor in the temperatures higher than 300 °C. It follows that hydrochars have higher thermal stability in this range. This hints to a partial cross-linking of the hydrochar molecule [16]. The highest mass loss was observed at a temperature around 500 °C for all materials. Subsequent increasing of the temperature cause flattening of TG curves and an almost complete decrease in the conversion rate DTG. Table A.1 shows the final residue obtained at 900 °C during thermogravimetric measurements. The pyrolysis yield at 900 °C for raw BSG was 19.91 wt. %. The HTC process applied before pyrolysis significantly increased the pyrolysis yields, final residues for hydrochars were 28.30, 40.68, and 45.75 wt. % for HTC-180-4, HTC-220-2, and HTC-220-4, respectively. Increasing the temperature and residence time of the hydrothermal carbonization process result in higher pyrolysis yields due to higher carbonization degree of hydrochars. On the other hand, the application of HTC as an additional process in the pyrolysis process line (Fig. 1, Scenario B) decrease the amount of feedstock for pyrolysis proportionally to the hydrothermal carbonization yield. The influence of the heating rate on the final yield is also investigated. A slower heating up results in an increased residence time of the volatiles inside the particle of the biomass. It results in higher char yield due to secondary char formation (cracking, re-polymerization and re-condensation reactions) [53–55]. This effect is observed when comparing slow pyrolysis (0.1-2 °C s<sup>-1</sup>) which focused on biochar production, and flash pyrolysis (>1000 °C s<sup>-1</sup>) which focus on bio-oil production [56]. In this study

applied heating rates (5 to 40 °C min<sup>-1</sup>) were in the range of slow pyrolysis. However, increasing the heating rate results in slightly higher final char yield. It may be due to the heat transfer limitation caused by a significant difference in residence time (20 min to 160 min) for samples carried out with different heating rates. The temperature sensor in TGA indicates the temperature inside the furnace instead of the exact temperature of the measured sample. Higher heating rates may cause that the sample is not able to heat up so fast due to shorter heating time. As a result, the sample has a lower temperature what leads to slightly higher char yield. As a consequence of the heat transfer, the heating rate also affects the temperature dependence of degradation. When increasing the heating rate, the temperature corresponding to the characteristic peaks (DTG) is higher (shifted to the right). This trend corresponds to other scientists investigating thermogravimetric decomposition of biomass [24,25,27,28,49]. Besides, a higher heating rate causes faster decomposition rates of the material due to the shorter time needed to reach the same final temperature.

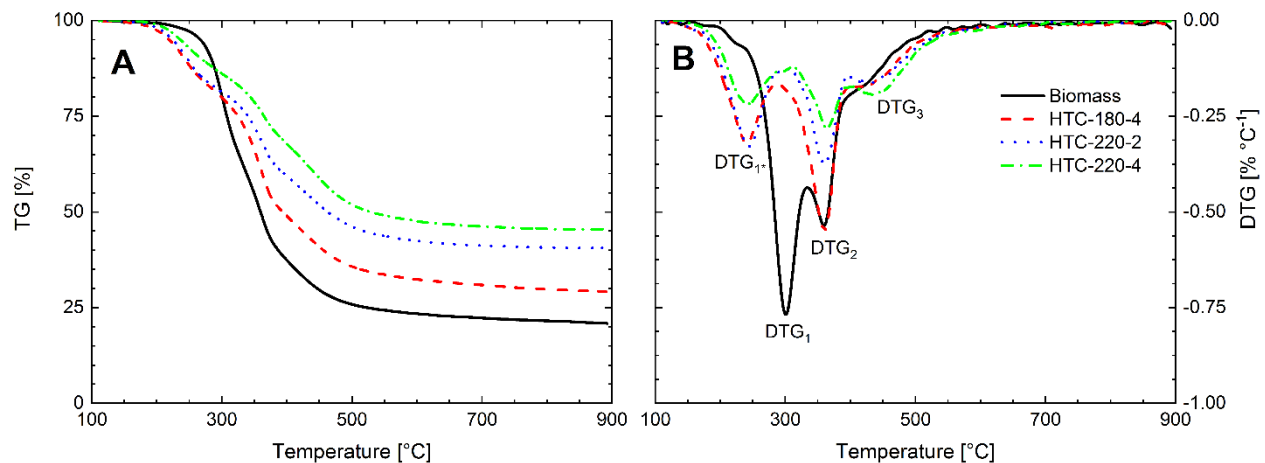


**Fig. 3.** A-TG and B-DTG curves for BSG and hydrochars, heating rate 20 [°C min<sup>-1</sup>].

### 3.4. Kinetics

Calculation of the kinetics according to the KAS method for BSG and hydrochars was carried out in the temperature range of 105 – 800 °C, for four heating rates 5, 10, 20 and 40 °C min<sup>-1</sup>. Linear fit plots for selected conversion degrees are shown in Fig. 4. The slope was used to calculate the activation energy for each conversion point. The obtained results with standard deviations and the temperature profiles were presented in Fig. 5.

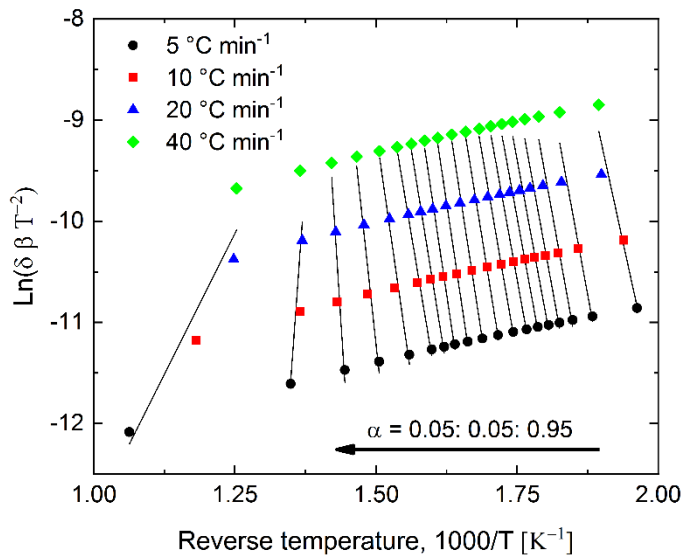


**Fig. 4.** Linear fit plots using KAS method to determine the activation energy for BSG.

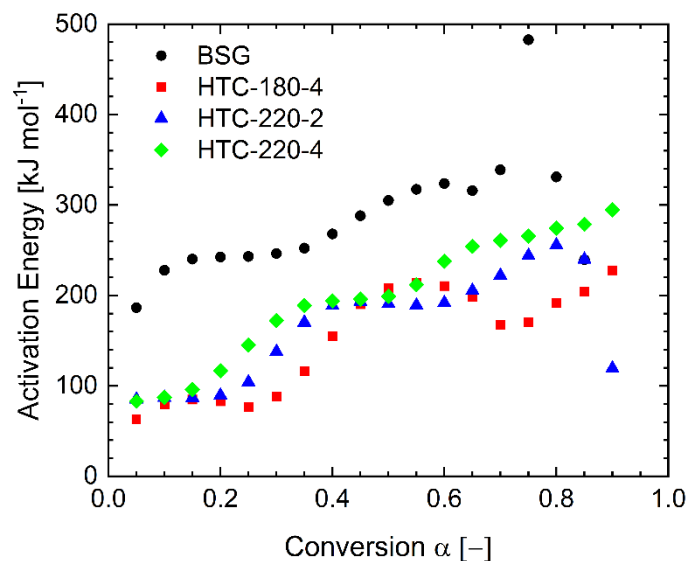


Fig. 5. Activation energies with standard deviation for A-BSG, B- HTC-180-4, C-HTC-220-2, D HTC-220-4.

The kinetic parameters are summarized in Table A.2. The apparent activation energy calculated in the conversion range of 5 to 85% for BSG took values from 187 to 338 with an average of 285 kJ mol<sup>-1</sup>. The values obtained are similar to coffee ground residues (~190-353 kJ mol<sup>-1</sup>) published recently by Mašek et al. [27] and higher than those obtained for other biomasses, e.g., tobacco plant waste (118-257 kJ mol<sup>-1</sup>) [57] and rice husk (221-229 kJ mol<sup>-1</sup>) [58]. On the other hand, the activation energies calculated for hydrochars are in the range of 63-214, 85-256 and 83-279 kJ mol<sup>-1</sup> for HTC-180-4, HTC-220-2, and HTC-220-4, respectively. It follows that the activation energy for hydrochars is lower than for the precursor. Recently published research about pyrolysis kinetic of hydrochar by Hameed et al. [28] showed activation energy (91-163 kJ mol<sup>-1</sup>) for hydrochar produced at 200 °C during 5 hours residence time from Karanji fruit hulls. These values were higher than initial biomass (28-93 kJ mol<sup>-1</sup>). However, the obtained values for biomass seem to be very low. The average activation energies presented by Li et al. [49] for hydrochars produced from sawdust were in the range of 150 to 195 kJ mol<sup>-1</sup>, which gives similar results obtained in this study 147, 170 and 188 kJ mol<sup>-1</sup> for HTC-180-4, HTC-220-2, and HTC-220-4,

respectively. The differences can arise due to use of different biomasses, heating rates, and final temperatures during the experiments as well as the complexity of the pyrolysis process.

The lower activation energy for hydrochars may confirm the fact that the thermochemical conversion occurring in wet conditions (HTC or wet torrefaction) proceeds according to different mechanisms than dry processing (torrefaction). It also results in a faster mass loss in the initial stage of pyrolysis at rather low temperatures (up to 300 °C) related with DTG<sub>1</sub>\* peaks. The much lower activation energy for hydrochars (below 90 kJ mol<sup>-1</sup>) at the initial stages of conversion, comprising up to ca. 30% compared to biomass (187 kJ mol<sup>-1</sup>) may be caused by the absence of hemicellulose in hydrochars which was hydrolyzed during HTC. A characteristic bulge appears for all materials in the conversion range from 0.4 to 0.7. The conversion 0.4 corresponds to a temperature around 350 °C which is related to the decomposition of cellulose (peak DTG<sub>2</sub>). For HTC-180-4 the convexity is visible with the highest intensity; it could be caused by the high cellulose content, which has not been converted because of the low temperature in the HTC process. For two other chars, the bulge decreased, it would confirm the effect of cellulose, which in this case has been significantly converted. Also, it can be observed that the standard deviation of biomass is much higher compared to hydrochars. It may be due to the high heterogeneity and the disorder of the biomass structure which is changed during the hydrothermal carbonization process, where the new material is formed during polymerization of intermediates products such as 5-HMF [9,16].

To summarize the pyrolysis kinetics, it is necessary to specify the pre-exponential factor (A), which explain reaction chemistry (defines the frequency of collisions of two molecules in collision theory). As previously mentioned, the pyrolysis process is characterized by high complexity and the mechanisms is not clearly defined. Herein, the A factor was estimated based

on Eq. 10, which uses the temperature corresponding to the largest DTG peak. The values of parameter A ( $s^{-1}$ ) for BSG are in the range of  $10^{12}$ - $10^{29}$  for conversions up to 70%, then increase very rapidly to  $10^{166}$ . Such a massive difference may result from an instability of the method in this range (low  $R^2$  value =0.59). For hydrochars, these values are  $10^2$ - $10^{14}$  for HTC-180-4 and  $10^4$ - $10^{21}$  for both hydrochar produced at 220 °C. According to Turmanova et al., [59] A-values higher than  $10^9$  characterize a more straightforward complex, lower values show the surface or closed system reaction. The literature values of pre-exponential factor A for different biomasses are  $10^{10}$ - $10^{15}$  for bulrush [24],  $10^7$ - $10^{12}$  for rice straw,  $10^3$ - $10^{21}$  for switchgrass [25] and  $10^3$ - $10^{10}$  for hydrochar (Karanj fruit hulls) [28]. Parameters describing the kinetics (activation energy and pre-exponential factor) are instrumental in understanding the pyrolysis process. With this information, it is possible to get an overview of the progression of the hydrochars pyrolysis.

The ranges given in the literature for TG results are rather high, but in this study, it can be concluded that for hydrochar the activation energy and the Arrhenius factor are lower than for the original biomass. This can be explained by the different structure. Biomass properties are strongly determined by carbohydrates, as main components. Carbohydrates are by C-O bonds connected sugar molecules. The single chains, especially in the case of cellulose, are stabilized by hydrogen bonds. This leads to a relative high thermal stability, expressed as a rather high activation energy in TGA. In hydrochar, the situation is completely different. During hydrothermal conversion, carbohydrates are hydrolyzed easily and at low temperature. The sugars are solved and shows further reactions like water elimination and polymerization ([10] and literature cited therein). The structure formed can be characterized as a complex polymer from Furfurals [60], which is not able to form hydrogen bonds to stabilize the single chains. At increased HTC temperature and after thermal treatment, crosslinking occurs, which leads to a stronger stabilization than hydrogen bonds. In simple words: Low temperature hydrochar can melt and evaporate, carbohydrates not, because

of the hydrogen bonds. Evaporation and perhaps some bond splitting is enough to produce a mass reduction in TGA, or leads to low activation energies, after KAS analysis.

Usually, also here, activation energies are given in molar quantities. The reason is, that the Arrhenius equation was originally developed for gases, not for solids. This is also done here, to be able to compare results gained here with literature data. In contrast, the experiments are done, also like usually, on mass base. The molar mass for the biomass and the hydrochar is unknown. One possibility to come out of this dilemma is calculating an activation temperature ( $T_A$ , Table 4) instead of a molar activation energy [61].

Using the KAS model-free method is possible to calculate this data without accurate knowledge about the reaction mechanisms that occur in complex processes such as pyrolysis. The kinetic parameters allow for the establishment of the base models for the development of the chemical reactors (CFD modeling) providing necessary knowledge related to the decomposition of the material at elevated temperatures during the time. It can also be used for consecutive scaling up as well as the further process optimization (for example, process simulation software Aspen Plus) to maximize the yields and minimize the energy consumption of the process.

### 3.5. Heat flow during pyrolysis reaction (DSC)

DSC curves indicating heat flow during pyrolysis of BSG and hydrochars are shown in Fig. 6. Biomass and hydrochar produced in 180 °C are characterized by positive heat flow which indicates the exothermic reactions occurring during the pyrolysis process. The exothermic effect of biomass pyrolysis was published in reviews by Antal et al.[62] and Di Stasi et al. [63]. On the other hand, both hydrochar obtained in 220 °C show a negative heat flow which reflects the endothermic effect. It confirms the rule that generally pyrolysis in small scale (mg) is endothermic [64–67]. The DSC curve for HTC-180-4 is more similar to biomass than other hydrochars. It may be due to the lack of cellulose conversion during HTC and it affects that the hydrochar produced from biomass at 180 °C is not completely carbonized. Despite the conversion of hemicellulose, it resembles the precursor with the initiated phase of conversion into a hydrochar. Also, the DSC curves for hydrochars produced at 220 °C confirms that new material has been synthesized.

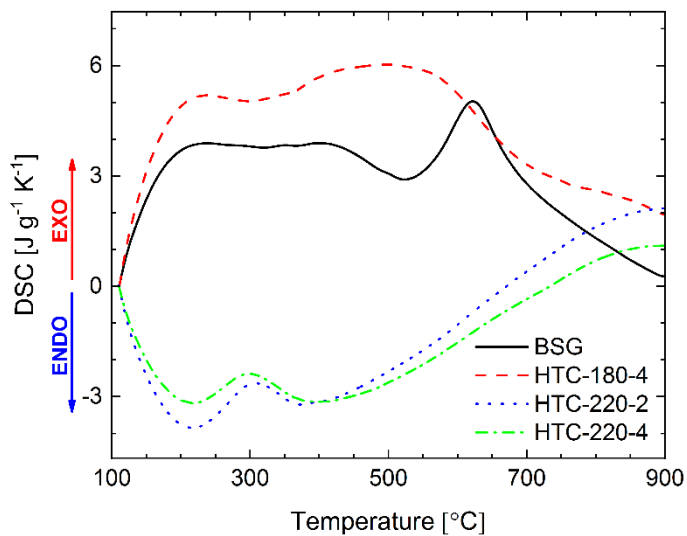


**Fig. 6.** Heat flow during pyrolysis of BSG and hydrochars at heating rate 20 °C min<sup>-1</sup>.

#### **4. Conclusion**

The study aimed to calculate kinetic parameters for pyrolysis of brewer's spent grains and hydrochars. The non-isothermal thermogravimetric analysis with four heating rates (5, 10, 20, 40 °C min<sup>-1</sup>) was performed. The Kissinger-Akahira-Sunose method was used to determine apparent activation energy ( $E_A$ ). The calculated average activation energies were 285, 147, 170 and 188 kJ mol<sup>-1</sup> for BSG, HTC-180-4, HTC-220-2, and HTC-220-4, respectively. From DTG curves it was found that hemicellulose is converted in the HTC process at 180 °C, while cellulose stayed unreacted. The decomposition of cellulose was observed for hydrochars produced at 220 °C. Additionally, a series of pyrolysis experiment at 300, 500, 700, and 900°C were conducted using TGA. The effect of the HTC process condition on the pyrochars yield was observed. Generally, the pyrolysis yield was higher for hydrochars than the precursor. Increasing the HTC condition results in higher pyrolysis yield at 900 °C, the yields were 22.0, 28.3, 37.4, 45.8% for BSG, HTC-180-4, HTC-220-2, and HTC-220-4, respectively. Higher pyrolysis yield and lower activation energies for hydrochars produced from brewer's spent grains show that HTC process preceding pyrolysis can extend the range of wet biomasses for bio-refinery purposes. It was observed that increasing pyrolysis temperature shift the chars into more carbonized (anthracites) range due to cross-linking and higher aromatization caused by the process. The H/C and O/C ratios for biomass and hydrochars pyrolyzed at the same temperature are very similar. Also, the volatiles released during pyrolysis were analyzed by Pyro GC-MS. The different composition of pyrolysis gases was detected. BSG released more phenolic derivative compounds while hydrochar produced more furans as well as other cyclic oxygen compounds.

#### **Acknowledgments**

This project has received funding from the European Union's Horizon 2020 research and innovation programme under the Marie Skłodowska-Curie grant agreement No 721991.

## Appendix A

**Table A.1**

*Characteristic parameters during thermal decomposition of brewer's spent grains and its hydrochars at different heating rates.*

Material	Heating rate °C min <sup>-1</sup>	T <sub>1</sub> , T <sub>1</sub> * °C	DTG <sub>1</sub> % °C <sup>-1</sup>	T <sub>2</sub> °C	DTG <sub>2</sub> % °C <sup>-1</sup>	T <sub>3</sub> , T <sub>3</sub> * °C	DTG <sub>3</sub> % °C <sup>-1</sup>	Final Residue % wt.
BSG	5	281.2	-0.687	340.5	-0.523	367.5	-0.198	18.98
	10	289.4	-0.736	349.6	-0.503	378.3	-0.202	19.24
	20	298.6	-0.776	357.9	-0.515	388.3	-0.211	20.99
	40	304.4	-0.887	358.3	-0.630	402.5	-0.228	20.44
	<b>average</b>	<b>293.4</b>	<b>-0.771</b>	<b>351.6</b>	<b>-0.543</b>	<b>384.2</b>	<b>-0.210</b>	<b>19.91</b>
HTC-180-4	5	211.2	-0.285	339.8	-0.592	404.2	-0.169	24.97
	10	223.9	-0.267	349.4	-0.556	412.1	-0.165	29.78
	20	236.0	-0.320	358.6	-0.543	422.3	-0.172	29.37
	40	251.6	-0.317	362.2	-0.633	419.9	-0.183	29.08
	<b>average</b>	<b>230.7</b>	<b>-0.297</b>	<b>352.5</b>	<b>-0.581</b>	<b>414.6</b>	<b>-0.172</b>	<b>28.30</b>
HTC-220-2	5	213.0	-0.268	340.1	-0.411	410.0	-0.168	38.71
	10	225.8	-0.276	353.3	-0.414	415.8	-0.162	39.54
	20	243.3	-0.325	359.5	-0.370	427.0	-0.167	41.32
	40	269.1	-0.326	378.3	-0.426	423.7	-0.155	43.17
	<b>average</b>	<b>237.8</b>	<b>-0.298</b>	<b>357.8</b>	<b>-0.405</b>	<b>419.1</b>	<b>-0.163</b>	<b>40.68</b>
HTC-220-4	5	209.2	-0.171	342.8	-0.298	410.3	-0.193	44.62
	10	221.3	-0.175	353.9	-0.302	427.4	-0.194	45.60
	20	243.9	-0.216	361.8	-0.279	436.4	-0.192	46.13
	40	269.4	-0.236	378.9	-0.340	441.1	-0.176	46.66
	<b>average</b>	<b>236.0</b>	<b>-0.199</b>	<b>359.4</b>	<b>-0.305</b>	<b>428.8</b>	<b>-0.189</b>	<b>45.75</b>

**Table A.2***Summary of the kinetic parameters for brewer's spent grains and its hydrochars.*

$\alpha$ -	$E_A$ kJ mol <sup>-1</sup>	$R^2$ -	$A$ s <sup>-1</sup>	$T_A$ K 10 <sup>3</sup>	$E_A$ kJ mol <sup>-1</sup>	$R^2$ -	$A$ s <sup>-1</sup>	$T_A$ K 10 <sup>3</sup>
<b>Material</b>	<b>BSG</b>				<b>HTC-180-4</b>			
0.05	186.50	0.81	1.17E+12	22.43	62.89	0.79	9.05E+02	7.56
0.10	227.85	0.88	1.66E+18	27.41	79.24	0.87	2.72E+04	9.53
0.15	240.19	0.93	1.34E+20	28.89	84.80	0.91	8.50E+04	10.20
0.20	242.52	0.95	3.54E+20	29.17	82.86	0.89	5.68E+04	9.97
0.25	243.15	0.97	4.64E+20	29.25	76.83	0.79	1.57E+04	9.24
0.30	246.34	0.98	9.45E+20	29.63	88.18	0.74	1.37E+05	10.61
0.35	252.30	0.98	3.44E+21	30.35	116.50	0.76	3.77E+07	14.01
0.40	267.98	0.98	9.68E+22	32.23	154.98	0.81	7.63E+10	18.64
0.45	288.12	0.98	8.09E+24	34.65	190.25	0.87	9.41E+13	22.88
0.50	305.07	0.98	3.14E+26	36.69	208.11	0.90	3.57E+15	25.03
0.55	317.36	0.98	3.92E+27	38.17	213.69	0.93	1.12E+16	25.70
0.60	323.89	0.98	1.60E+28	38.96	210.42	0.93	6.01E+15	25.31
0.65	315.99	0.98	2.96E+27	38.01	198.37	0.91	5.78E+14	23.86
0.70	338.78	0.96	3.64E+29	40.75	167.24	0.77	1.15E+12	20.12
0.75	482.71	0.82	4.30E+43	58.06	170.34	0.72	1.38E+12	20.49
0.80	331.10	0.59	3.34E+69	39.82	191.85	0.74	5.42E+13	23.08
0.85	239.62	0.59	1.72E+166	28.82	204.37	0.77	2.15E+14	24.58
<b>average</b>	<b>285.26</b>	<b>0.90</b>	<b>-</b>	<b>34.31</b>	<b>147.11</b>	<b>0.83</b>	<b>-</b>	<b>17.69</b>
<b>Material</b>	<b>HTC-220-2</b>				<b>HTC-220-4</b>			
0.05	85.19	0.98	9.98E+04	10.25	78.39	0.99	4.25E+04	9.43
0.10	87.22	0.99	1.30E+05	10.49	82.98	0.99	1.10E+05	9.98
0.15	86.77	0.99	1.15E+05	10.44	91.69	0.98	6.47E+05	11.03
0.20	89.62	0.98	2.06E+05	10.78	112.46	0.95	4.14E+07	13.53
0.25	104.21	0.96	4.43E+06	12.53	142.34	0.91	1.56E+10	17.12
0.30	137.92	0.93	5.40E+09	16.59	167.08	0.92	2.07E+12	20.10
0.35	170.20	0.93	3.53E+12	20.47	183.23	0.95	5.01E+13	22.04
0.40	188.88	0.96	1.14E+14	22.72	189.07	0.97	1.60E+14	22.74
0.45	193.33	0.98	2.05E+14	23.25	191.74	0.98	2.75E+14	23.06
0.50	190.65	0.98	1.09E+14	22.93	194.98	0.97	5.26E+14	23.45
0.55	189.12	0.98	7.75E+13	22.75	208.77	0.94	7.90E+15	25.11
0.60	191.91	0.98	1.39E+14	23.08	235.17	0.88	1.40E+18	28.29
0.65	205.44	0.89	5.49E+15	24.71	251.28	0.89	3.31E+19	30.22
0.70	222.05	0.76	3.69E+17	26.71	258.15	0.91	1.29E+20	31.05
0.75	244.16	0.74	5.03E+19	29.37	263.15	0.92	3.51E+20	31.65
0.80	255.68	0.73	1.31E+21	30.75	273.82	0.92	2.88E+21	32.93
0.85	239.95	0.63	2.18E+21	28.86	279.40	0.90	8.81E+21	33.61
<b>average</b>	<b>169.55</b>	<b>0.90</b>	<b>-</b>	<b>20.39</b>	<b>188.45</b>	<b>0.94</b>	<b>-</b>	<b>22.67</b>

## Literature

- [1] Statista, Beer Production Worldwide From 1998 to 2016, Stat. Portal. (2017). <https://www.statista.com/statistics/270275/worldwide-beer-production/> (accessed May 8, 2018).
- [2] Barth-Haas Group, The Barth Report, (2015) 32. doi:53093-1505-1002.
- [3] A.O. Balogun, F. Sotoudehniakarani, A.G. McDonald, Thermo-kinetic, spectroscopic study of brewer's spent grains and characterisation of their pyrolysis products, *J. Anal. Appl. Pyrolysis*. 127 (2017) 8–16. doi:10.1016/j.jaap.2017.09.009.
- [4] R. Ravindran, S. Jaiswal, N. Abu-Ghannam, A.K. Jaiswal, A comparative analysis of pretreatment strategies on the properties and hydrolysis of brewers' spent grain, *Bioresour. Technol.* 248 (2018) 272–279. doi:10.1016/j.biortech.2017.06.039.
- [5] A.L. McCarthy, Y.C. O'Callaghan, C.O. Piggott, R.J. FitzGerald, N.M. O'Brien, Brewers' spent grain; Bioactivity of phenolic component, its role in animal nutrition and potential for incorporation in functional foods: A review, *Proc. Nutr. Soc.* 72 (2013) 117–125. doi:10.1017/S0029665112002820.
- [6] P. Niemi, T. Tamminen, A. Smeds, K. Viljanen, T. Ohra-Aho, U. Holopainen-Mantila, C.B. Faulds, K. Poutanen, J. Buchert, Characterization of lipids and lignans in brewer's spent grain and its enzymatically extracted fraction, *J. Agric. Food Chem.* 60 (2012) 9910–9917. doi:10.1021/jf302684x.
- [7] J. Poerschmann, B. Weiner, H. Wedwitschka, I. Baskyr, R. Koehler, F.D. Kopinke, Characterization of biocoals and dissolved organic matter phases obtained upon hydrothermal carbonization of brewer's spent grain, *Bioresour. Technol.* 164 (2014) 162–169. doi:10.1016/j.biortech.2014.04.052.
- [8] E. Mallen, V. Najdanovic-Visak, Brewers' spent grains: Drying kinetics and biodiesel production, *Bioresour. Technol. Reports*. 1 (2018) 16–23. doi:10.1016/j.biteb.2018.01.005.
- [9] A. Funke, F. Ziegler, Hydrothermal carbonization of biomass: A summary and discussion of chemical mechanisms for process engineering, *Biofuels, Bioprod. Biorefining*. 4 (2010) 160–177. doi:10.1002/bbb.198.
- [10] A. Kruse, N. Dahmen, Water - A magic solvent for biomass conversion, *J. Supercrit. Fluids*. 96 (2015) 36–45. doi:10.1016/j.supflu.2014.09.038.
- [11] X. Zhu, Y. Liu, F. Qian, S. Zhang, J. Chen, Investigation on the Physical and Chemical Properties of Hydrochar and Its Derived Pyrolysis Char for Their Potential Application: Influence of Hydrothermal Carbonization Conditions, *Energy and Fuels*. 29 (2015) 5222–5230. doi:10.1021/acs.energyfuels.5b00512.
- [12] Y. Shen, S. Yu, S. Ge, X. Chen, X. Ge, M. Chen, Hydrothermal carbonization of medical wastes and lignocellulosic biomass for solid fuel production from lab-scale to pilot-scale, *Energy*. 118 (2017) 312–323. doi:10.1016/j.energy.2016.12.047.
- [13] M.-M. Titirici, R.J. White, C. Falco, M. Sevilla, Black perspectives for a green future: hydrothermal carbons for environment protection and energy storage, *Energy Environ. Sci.* 5 (2012) 6796. doi:10.1039/c2ee21166a.
- [14] J.A. Libra, K.S. Ro, C. Kammann, A. Funke, N.D. Berge, Y. Neubauer, M.-M. Titirici, C. Fühner, O.

- Bens, J. Kern, K.-H. Emmerich, Hydrothermal carbonization of biomass residuals: a comparative review of the chemistry, processes and applications of wet and dry pyrolysis, *Biofuels*. 2 (2011) 71–106. doi:10.4155/bfs.10.81.
- [15] X. Cao, K.S. Ro, J.A. Libra, C.I. Kammann, I. Lima, N. Berge, A. Li, Y. Li, N. Chen, J. Yang, B. Deng, J. Mao, Effects of biomass types and carbonization conditions on the chemical characteristics of hydrochars, *J. Agric. Food Chem.* 61 (2013) 9401–9411. doi:10.1021/jf402345k.
- [16] A. Kruse, T. Zevaco, Properties of Hydrochar as Function of Feedstock, Reaction Conditions and Post-Treatment, *Energies*. 11 (2018) 674. doi:10.3390/en11030674.
- [17] X. Zhao, G. Becker, N. Faweya, C.R. Correa, S. Yang, X. Xie, A. Kruse, Biomass Conversion and Biorefinery Fertilizer and Activated Carbon Production by Hydrothermal Carbonization of Digestate, *Biomass Convers. Biorefinery*. (2017).
- [18] M. Ulbrich, D. Preßl, S. Fendt, M. Gaderer, H. Spliethoff, Impact of HTC reaction conditions on the hydrochar properties and CO<sub>2</sub> gasification properties of spent grains, *Fuel Process. Technol.* 167 (2017) 663–669. doi:10.1016/j.fuproc.2017.08.010.
- [19] R.K. Garlapalli, B. Wirth, M.T. Reza, Pyrolysis of hydrochar from digestate: Effect of hydrothermal carbonization and pyrolysis temperatures on pyrochar formation, *Bioresour. Technol.* 220 (2016) 168–174. doi:10.1016/j.biortech.2016.08.071.
- [20] M. Breulmann, M. van Afferden, R.A. Müller, E. Schulz, C. Fühner, Process conditions of pyrolysis and hydrothermal carbonization affect the potential of sewage sludge for soil carbon sequestration and amelioration, *J. Anal. Appl. Pyrolysis*. 124 (2017) 256–265. doi:10.1016/j.jaap.2017.01.026.
- [21] P. Arauzo, M. Olszewski, A. Kruse, Hydrothermal Carbonization Brewer's Spent Grains with the Focus on Improving the Degradation of the Feedstock, *Energies*. 11 (2018). doi:10.3390/en11113226.
- [22] J. Cai, D. Xu, Z. Dong, X. Yu, Y. Yang, S.W. Banks, A. V. Bridgwater, Processing thermogravimetric analysis data for isoconversional kinetic analysis of lignocellulosic biomass pyrolysis: Case study of corn stalk, *Renew. Sustain. Energy Rev.* 82 (2018) 2705–2715. doi:10.1016/j.rser.2017.09.113.
- [23] M. Carrier, L. Auret, A. Bridgwater, J.H. Knoetze, Using Apparent Activation Energy as a Reactivity Criterion for Biomass Pyrolysis, *Energy and Fuels*. 30 (2016) 7834–7841. doi:10.1021/acs.energyfuels.6b00794.
- [24] M.S. Ahmad, M.A. Mehmood, S.T.H. Taqvi, A. Elkamel, C.G. Liu, J. Xu, S.A. Rahimuddin, M. Gull, Pyrolysis, kinetics analysis, thermodynamics parameters and reaction mechanism of *Typha latifolia* to evaluate its bioenergy potential, *Bioresour. Technol.* 245 (2017) 491–501. doi:10.1016/j.biortech.2017.08.162.
- [25] Y. Xu, B. Chen, Investigation of thermodynamic parameters in the pyrolysis conversion of biomass and manure to biochars using thermogravimetric analysis, *Bioresour. Technol.* 146 (2013) 485–493. doi:10.1016/j.biortech.2013.07.086.
- [26] S.A. Channiwala, P.P. Parikh, A unified correlation for estimating HHV of solid, liquid and gaseous fuels, *Fuel*. 81 (2002) 1051–1063. doi:https://doi.org/10.1016/S0016-2361(01)00131-4.
- [27] J. Feroso, O. Mašek, Thermochemical decomposition of coffee ground residues by TG-MS: A kinetic study, *J. Anal. Appl. Pyrolysis*. 130 (2018) 249–255. doi:10.1016/j.jaap.2017.12.007.

- [28] M.A. Islam, M. Asif, B.H. Hameed, Pyrolysis kinetics of raw and hydrothermally carbonized Karanj (*Pongamia pinnata*) fruit hulls via thermogravimetric analysis, *Bioresour. Technol.* 179 (2015) 227–233. doi:10.1016/j.biortech.2014.11.115.
- [29] R. Ebrahimi-Kahrizsangi, M.H. Abbasi, Evaluation of reliability of Coats-Redfern method for kinetic analysis of non-isothermal TGA, *Trans. Nonferrous Met. Soc. China (English Ed.)* 18 (2008) 217–221. doi:10.1016/S1003-6326(08)60039-4.
- [30] A.W. COATS, J.P. REDFERN, Kinetic Parameters from Thermogravimetric Data, *Nature.* 201 (1964) 68. <http://dx.doi.org/10.1038/201068a0>.
- [31] H.E. Kissinger, Reaction Kinetics in Differential Thermal Analysis, *Anal. Chem.* 29 (1957) 1702–1706. doi:10.1021/ac60131a045.
- [32] H.L. Friedman, Kinetics of thermal degradation of char-forming plastics from thermogravimetry. Application to a phenolic plastic, *J. Polym. Sci. Polym. Symp.* 6 (1964) 183–195.
- [33] T. Ozawa, A New Method of Analyzing Thermogravimetric Data, *Bull. Chem. Soc. Jpn.* 38 (1965) 1881–1886. doi:10.1246/bcsj.38.1881.
- [34] J.H. Flynn, L.A. Wall, A quick, direct method for the determination of activation energy from thermogravimetric data, *J. Polym. Sci. Part B Polym. Lett.* 4 (2018) 323–328. doi:10.1002/pol.1966.110040504.
- [35] T. Akahira, T. Sunose, Joint convention of four electrical institutes, *Res. Rep. Chiba Inst. Technol. (Sci. Technol.)*. 16 (1971) 22–31.
- [36] Y. gan Liang, B. Cheng, Y. bin Si, D. ju Cao, H. yang Jiang, G. min Han, X. hong Liu, Thermal decomposition kinetics and characteristics of *Spartina alterniflora* via thermogravimetric analysis, *Renew. Energy.* 68 (2014) 111–117. doi:10.1016/j.renene.2014.01.041.
- [37] S.H. Kim, Investigation of Thermodynamic Parameters in the Thermal Decomposition of Plastic Waste - Waste Lube Oil Compounds, 44 (2010) 5313–5317.
- [38] R. Huang, C. Fang, X. Lu, R. Jiang, Y. Tang, Transformation of Phosphorus during (Hydro)thermal Treatments of Solid Biowastes: Reaction Mechanisms and Implications for P Reclamation and Recycling, *Environ. Sci. Technol.* 51 (2017) 10284–10298. doi:10.1021/acs.est.7b02011.
- [39] S.M. Heilmann, J.S. Molde, J.G. Timler, B.M. Wood, A.L. Mikula, G. V. Vozhdayev, E.C. Colosky, K.A. Spokas, K.J. Valentas, Phosphorus reclamation through hydrothermal carbonization of animal manures, *Environ. Sci. Technol.* 48 (2014) 10323–10329. doi:10.1021/es501872k.
- [40] T. Wang, Y. Zhai, Y. Zhu, C. Peng, B. Xu, T. Wang, C. Li, G. Zeng, Influence of temperature on nitrogen fate during hydrothermal carbonization of food waste, *Bioresour. Technol.* 247 (2018) 182–189. doi:<https://doi.org/10.1016/j.biortech.2017.09.076>.
- [41] P. Fu, S. Hu, J. Xinag, L. Sun, T. Yang, A. Zhang, Y. Wang, G. Chen, Effects of Pyrolysis Temperature on Characteristics of Porosity in Biomass Chars, in: 2009 Int. Conf. Energy Environ. Technol., 2009: pp. 109–112. doi:10.1109/ICEET.2009.33.
- [42] W. Yang, H. Wang, M. Zhang, J. Zhu, J. Zhou, S. Wu, Fuel properties and combustion kinetics of hydrochar prepared by hydrothermal carbonization of bamboo, *Bioresour. Technol.* 205 (2016) 199–204. doi:<https://doi.org/10.1016/j.biortech.2016.01.068>.
- [43] Q.-V. Bach, K.-Q. Tran, Dry and Wet Torrefaction of Woody Biomass – A Comparative Study on

- Combustion Kinetics, *Energy Procedia*. 75 (2015) 150–155.  
doi:<https://doi.org/10.1016/j.egypro.2015.07.270>.
- [44] G. Agegnehu, A.K. Srivastava, M.I. Bird, The role of biochar and biochar-compost in improving soil quality and crop performance: A review, *Appl. Soil Ecol.* 119 (2017) 156–170.  
doi:<https://doi.org/10.1016/j.apsoil.2017.06.008>.
- [45] K. Sun, J. chun Jiang, Preparation and characterization of activated carbon from rubber-seed shell by physical activation with steam, *Biomass and Bioenergy*. 34 (2010) 539–544.  
doi:10.1016/j.biombioe.2009.12.020.
- [46] K. Mochizuki, F. Soutric, K. Tadokoro, M.J. Antal, M. Tóth, B. Zelei, G. Várhegyi, Electrical and Physical Properties of Carbonized Charcoals, *Ind. Eng. Chem. Res.* 42 (2003) 5140–5151.  
doi:10.1021/ie030358e.
- [47] S. Herou, P. Schlee, A.B. Jorge, M. Titirici, Biomass-derived electrodes for flexible supercapacitors, *Curr. Opin. Green Sustain. Chem.* 9 (2018) 18–24.  
doi:<https://doi.org/10.1016/j.cogsc.2017.10.005>.
- [48] M. Olszewski, R.S. Kempegowda, Ø. Skreiberg, L. Wang, T. Løvås, Techno-Economics of Biocarbon Production Processes under Norwegian Conditions, *Energy & Fuels*. 31 (2017) 14338–14356.  
doi:10.1021/acs.energyfuels.6b03441.
- [49] H. Li, S. Wang, X. Yuan, Y. Xi, Z. Huang, M. Tan, C. Li, The effects of temperature and color value on hydrochars' properties in hydrothermal carbonization, *Bioresour. Technol.* 249 (2018) 574–581. doi:<https://doi.org/10.1016/j.biortech.2017.10.046>.
- [50] M.T. Reza, B. Wirth, U. Lüder, M. Werner, Behavior of selected hydrolyzed and dehydrated products during hydrothermal carbonization of biomass, *Bioresour. Technol.* 169 (2014) 352–361.  
doi:<https://doi.org/10.1016/j.biortech.2014.07.010>.
- [51] J. Shen, C. Igathinathane, M. Yu, A.K. Pothula, Biomass pyrolysis and combustion integral and differential reaction heats with temperatures using thermogravimetric analysis/differential scanning calorimetry, *Bioresour. Technol.* 185 (2015) 89–98. doi:10.1016/j.biortech.2015.02.079.
- [52] L. Dai, C. He, Y. Wang, Y. Liu, R. Ruan, Z. Yu, Y. Zhou, D. Duan, L. Fan, Y. Zhao, Hydrothermal pretreatment of bamboo sawdust using microwave irradiation, *Bioresour. Technol.* 247 (2018) 234–241. doi:<https://doi.org/10.1016/j.biortech.2017.08.104>.
- [53] J.E. White, W.J. Catallo, B.L. Legendre, Biomass pyrolysis kinetics: A comparative critical review with relevant agricultural residue case studies, *J. Anal. Appl. Pyrolysis*. 91 (2011) 1–33.  
doi:<https://doi.org/10.1016/j.jaap.2011.01.004>.
- [54] Z. Shuping, W. Yulong, Y. Mingde, L. Chun, T. Junmao, Pyrolysis characteristics and kinetics of the marine microalgae *Dunaliella tertiolecta* using thermogravimetric analyzer, *Bioresour. Technol.* 101 (2010) 359–365. doi:<https://doi.org/10.1016/j.biortech.2009.08.020>.
- [55] H. Haykiri-Acma, S. Yaman, S. Kucukbayrak, Effect of heating rate on the pyrolysis yields of rapeseed, *Renew. Energy*. 31 (2006) 803–810. doi:<https://doi.org/10.1016/j.renene.2005.03.013>.
- [56] J. Feroso, P. Pizarro, J.M. Coronado, D.P. Serrano, Transportation Biofuels via the Pyrolysis Pathway: Status and Prospects BT - Encyclopedia of Sustainability Science and Technology, in: R.A. Meyers (Ed.), Springer New York, New York, NY, 2017: pp. 1–33. doi:10.1007/978-1-4939-2493-6\_963-1.

- [57] W. Wu, Y. Mei, L. Zhang, R. Liu, J. Cai, Kinetics and reaction chemistry of pyrolysis and combustion of tobacco waste, *Fuel*. 156 (2015) 71–80. doi:<https://doi.org/10.1016/j.fuel.2015.04.016>.
- [58] R.M. Braga, D.M.A. Melo, F.M. Aquino, J.C.O. Freitas, M.A.F. Melo, J.M.F. Barros, M.S.B. Fontes, Characterization and comparative study of pyrolysis kinetics of the rice husk and the elephant grass, *J. Therm. Anal. Calorim.* 115 (2014) 1915–1920. doi:10.1007/s10973-013-3503-7.
- [59] S.C. Turmanova, S.D. Genieva, A.S. Dimitrova, L.T. Vlaev, Non-isothermal degradation kinetics of filled with rice husk ash polypropylene composites, *Express Polym. Lett.* 2 (2008) 133–146. doi:10.3144/expresspolymlett.2008.18.
- [60] C. Falco, N. Baccile, M.-M. Titirici, Morphological and structural differences between glucose, cellulose and lignocellulosic biomass derived hydrothermal carbons, *Green Chem.* 13 (2011) 3273–3281. doi:10.1039/C1GC15742F.
- [61] A. Kruse, F. Badoux, R. Grandl, D. Wüst, Hydrothermale Karbonisierung: 2. Kinetik der Biertreber-Umwandlung, *Chemie Ing. Tech.* 84 (2012) 509–512. doi:10.1002/cite.201100168.
- [62] M.J. Antal, M. Grønli, The Art, Science, and Technology of Charcoal Production, *Ind. Eng. Chem. Res.* 42 (2003) 1619–1640. doi:10.1021/ie0207919.
- [63] C. Di Blasi, C. Branca, A. Galgano, On the Experimental Evidence of Exothermicity in Wood and Biomass Pyrolysis, *Energy Technol.* 5 (2016) 19–29. doi:10.1002/ente.201600091.
- [64] A. Anca-Couce, R. Scharler, Modelling heat of reaction in biomass pyrolysis with detailed reaction schemes, *Fuel*. 206 (2017) 572–579. doi:<https://doi.org/10.1016/j.fuel.2017.06.011>.
- [65] C. Gomez, E. Velo, F. Barontini, V. Cozzani, Influence of Secondary Reactions on the Heat of Pyrolysis of Biomass, *Ind. Eng. Chem. Res.* 48 (2009) 10222–10233. doi:10.1021/ie9007985.
- [66] J. Rath, M.G. Wolfinger, G. Steiner, G. Krammer, F. Barontini, V. Cozzani, Heat of wood pyrolysis, *Fuel*. 82 (2003) 81–91. doi:[https://doi.org/10.1016/S0016-2361\(02\)00138-2](https://doi.org/10.1016/S0016-2361(02)00138-2).
- [67] A. Anca-Couce, N. Zobel, A. Berger, F. Behrendt, Smouldering of pine wood: Kinetics and reaction heats, *Combust. Flame*. 159 (2012) 1708–1719. doi:<https://doi.org/10.1016/j.combustflame.2011.11.015>.